

DEVELOPMENT OF CHARACTERIZATION TECHNIQUES FOR X-BAND ACCELERATOR STRUCTURES

S.M. Hanna, R.J. Loewen, H.A. Hoag, R.H. Miller, R.D. Ruth, J.W. Wang
Stanford Linear Accelerator Center, Stanford University, CA 94304 USA.

Abstract

The recent effort to develop accelerator structures for the Next Linear Collider (NLC), requires an accompanying development of accurate and efficient techniques to characterize these structures at different phases of development. At SLAC, we have been developing different microwave techniques to: verify predictions from computer simulations in the design phase, to insure that the machined cells are within the design tolerances, and finally, to confirm overall RF performance of the completed structure. For this final test, a semi-automated system was built to implement the bead-pulling technique under traveling-wave conditions. This technique maps the phase and amplitude of the axial electric field along the structure.

1 INTRODUCTION

At SLAC, we have built six (6) accelerator sections for the NLC Test Accelerator (NLCTA), [1]. These are nearly constant gradient structures employing Gaussian detuning as means of suppressing the transverse wakefields by varying the physical dimensions of successive cells. Four of these sections are Detuned Structures (DS). The other two are of the Damped Detuned Structure (DDS) type [2]. In these sections, further suppression of wakefields is done through damping of dipole modes excited by the beam. This is accomplished by means of four rectangular slots or manifolds equally spaced in azimuth around the cell and running the full length of the structure.

The DS sections include two 0.9m-long injector sections, and two 1.8m-long accelerator sections. In these four sections the assembly was done through brazing using copper/gold alloys. Variations in the braze fillet required fine tuning of individual cells after assembly.

The two 1.8m-long DDS sections were assembled using diffusion bonding, requiring no tuning. However, the existence of the manifold slots in the cell proper disturbs the azimuthal symmetry. Therefore, the design process included accurate frequency measurements of short stacks of sample cells. The data from these measurements were used to finalize the dimensions predicted from computer simulations.

In this paper, we discuss some of the techniques we use to characterize the above structures. In Figure 1, we outline the series of tests we have implemented to support different development phases of the accelerator sections

from the design phase, through manufacturing, and finally, testing of the complete accelerator section.

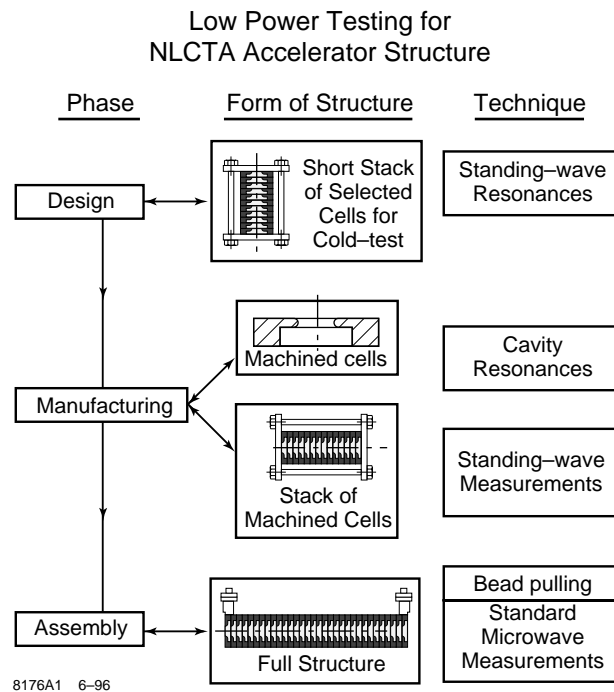


Figure 1. Outline of low-power microwave tests performed on NLCTA accelerator structures.

2 TESTS SUPPORTING DESIGN PHASE

During the design phase of DDS I, the accuracy of the simulation was tested by fabricating five (5) short stacks for cells 10, 70, 106, 156, and 196. Each stack consisted of five cells and two half cells of like dimensions. On-axis probes measure the accelerating mode frequency. Results of these measurements were used to refine the dimensions of the 204 cells of the structure predicted by computer simulation.

Off-axis, E-field probes in the manifolds are used to excite and detect dipole modes, while loop-type H-filed probes in the manifold are used to excite and detect manifold modes. Coupling between cell dipole modes and manifold modes can thus be characterized. Measured frequencies were found to agree well with the simulation. In Figure 2, we show the results of measurement (as compared to computer simulation) of the dispersion curves of the first and second dipole modes and the manifold mode in cell 106 of the DDS I section.

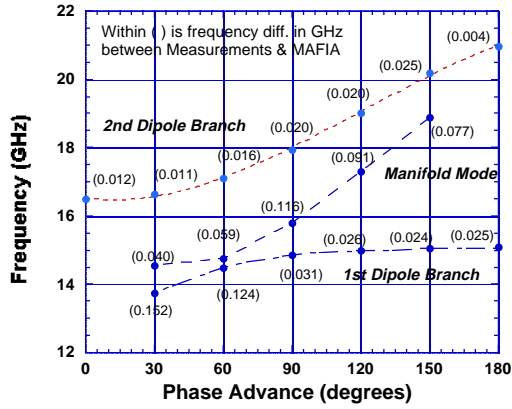


Figure 2. Measured dispersion relation for cell 106 of DDS I as compared to theoretical calculations.

3 TESTS DURING MANUFACTURING PHASE

3.1 Microwave QC of Cells

In all of the NLCTA structures, the diameter of each cell (2b), the thickness of its iris (t), and the diameter of its aperture (2a), all vary progressively from cell to cell. The goal is to detune the dipole modes and prevent short range cumulative build up of wakefields, while maintaining quasi-constant gradient characteristics of the fundamental accelerating mode [2]. To verify the regularity of machining of successive cells, we measured the resonant frequency of the individual cells using a setup for microwave quality control (QC), [3].

By plotting the inverse of the measured frequency versus the cell diameter, one obtains a straight line fit which is a convenient way of verifying the (2b) cell dimension. Results of measurement of 204 cells for DS II structure are depicted in Figure 3.

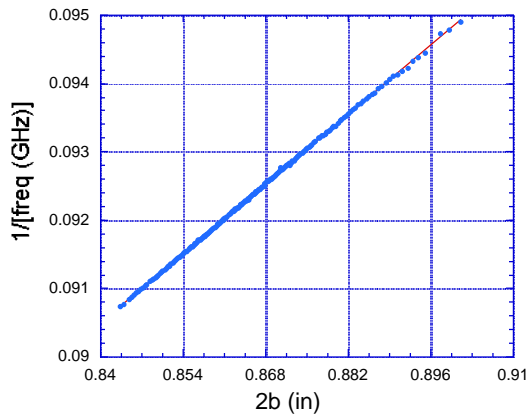


Figure 3. Measured 1/frequency versus cell diameter and the linear fit.

3.2 Tuning DS Sections

The four detuned structures were brazed and required tuning of the cells in the subassemblies. This is to correct for any deviations in the volume of the cells due to brazing. A stainless steel plunger is progressively pulled through the structure from the center of one cell to the next. The resulting phase shift is measured using an HP8510 Network Analyzer at the frequency corresponding to the operating frequency of 11.424 GHz and corrected for room temperature and dry N₂ under atmospheric pressure. Pushing or pulling the cylindrical walls of the cells affects the impedance match from cell to cell for the accelerating mode. Time-domain reflectometry (TDR) measurements are used to check on the matching as the tuning process progresses. The use of both frequency-domain and time-domain capabilities of the network analyzer proved effective in tuning the structure while monitoring the effect on the structure's match. In Figure 4, we show results of typical time-domain measurements during tuning. The reduction in reflection is apparent as more cells are tuned.

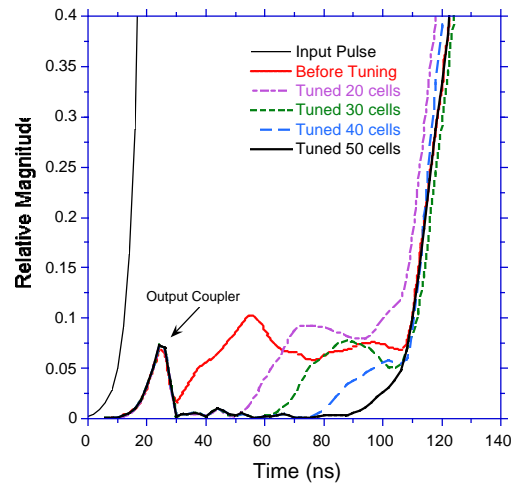


Figure 4 Results of time-domain reflection measurements at different tuning stages of DS II.

4 FULL STRUCTURE CHARACTERIZATION

Each of the completed accelerated sections was finally checked using a semi-automated system of bead-pull [3,4]. The technique implemented is based on traveling-wave perturbation [5]. Figure 5 shows a schematic for our bead-pull system. A small metallic cylindrical bead is attached to a thin nylon string along the axis of the vertically-mounted accelerator section. The position of the bead is determined by the position of the carriage moving on a lead screw driven by a stepper motor. The computer which controls the motor also collects and processes the reflection coefficient data (S_{11}) from the

microwave network analyzer which was operated in the fast acquisition mode. The measurement time is typically 3 minutes. The field perturbation introduced by the bead located at a given position can be modeled as a reactive discontinuity in a transmission line. The susceptance associated with this discontinuity is proportional to the energy perturbation, and hence to the square of the field at this location.

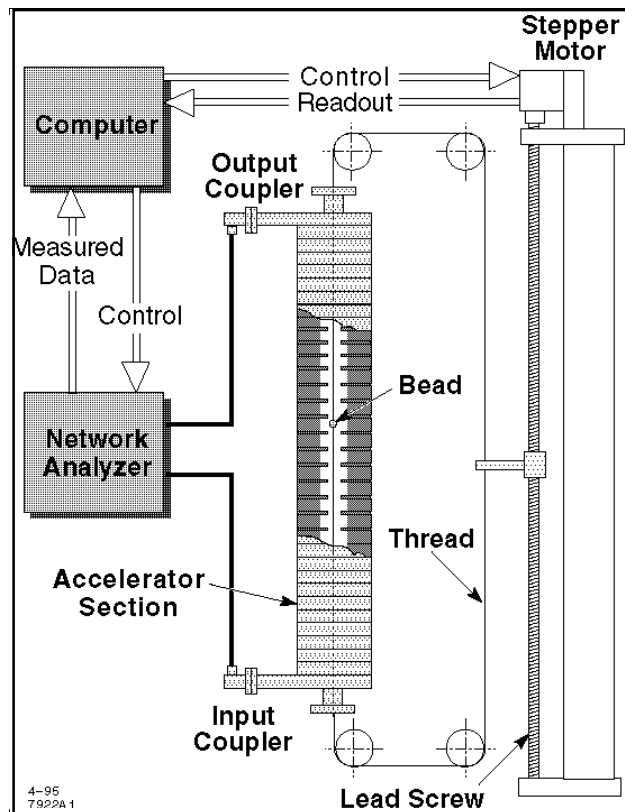


Figure 5. Schematic diagram for the semi-automated bead-pull test setup.

Using the bead-pull system shown schematically in Figure 5, we tested the 6 NLCTA accelerator sections. We used a stainless steel cylindrical bead of diameter $d_b=0.625$ mm and a length $l_b=1$ mm supported on a monofilament nylon string of diameter $d_s = 0.145$ mm. The measurements were made at frequencies corrected for the nylon string, the room temperature and dry N_2 . The variation in the reflection from the bead as it is pulled along the axis of each structure traces the hypotrochoid function. This trace can be predicted theoretically for a given longitudinal electric field, E_z based on its space harmonics. Our previous work, [4]

showed good agreement between theory and experiment. The electric field E_z can be obtained as the square root of the measured complex reflection coefficient (S_{11}). Measured E_z field for the DDS II section is shown in Figure 6. The three-fold symmetry of the accelerating $2\pi/3$ mode is manifested clearly.

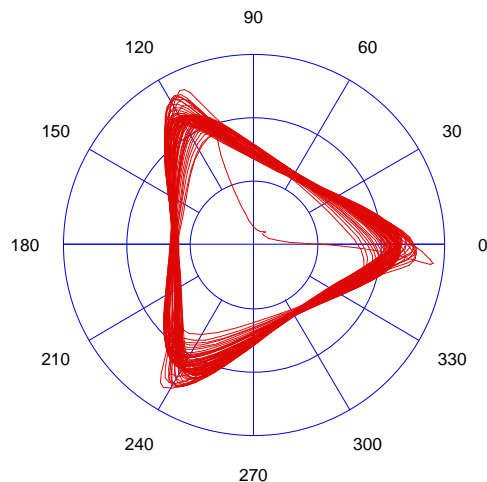


Figure 6. Phasor of the electric field along the axis of the DDS II accelerator section.

5 ACKNOWLEDGEMENTS

We thank K.Ko for the computer simulation data provided. This work is supported by Department of Energy contract DE-AC03-76SF00515.

REFERENCES

- [1] R. D. Ruth, "Results from the SLAC NLC Test Accelerator," in these proceedings
- [2] R. H. Miller, et al., "Damped Detuned Structure for the Next Linear Collider," Proc. of the XVII International Linear Accelerator Conference, pp 644 - 646.
- [3] S. M. Hanna, et al., "Microwave Cold-Testing Techniques for the NLC," Proceedings of the EPAC '96, pp 2056-2058.
- [4] S. M. Hanna, et al., "A Semi-Automated System for the Characterization of NLC Accelerating Structures," Proceeding of the 1995 Particle Accelerator Conf., pp 1108-1110.
- [5] K. B. Mallory and R. H. Miller, "On Nonresonant Perturbation Measurements," IEEE Trans. On Microwave Theory and Techniques, Vol. MTT-14, No. 1966, pp 99-100.